Water Splitting

Deutsche Ausgabe: DOI: 10.1002/ange.201600918
Internationale Ausgabe: DOI: 10.1002/anie.201600918

Synergistic Cocatalytic Effect of Carbon Nanodots and Co_3O_4 Nanoclusters for the Photoelectrochemical Water Oxidation on Hematite

*Peng Zhang[+], Tuo Wang[+], Xiaoxia Chang, Lei Zhang, and Jinlong Gong**

Abstract: *Cocatalysis plays an important role in enhancing the activity of semiconductor photocatalysts for solar water splitting. Compared to a single cocatalyst configuration, a cocatalytic system consisting of multiple components with different functions may realize outstanding enhancement through their interactions, yet limited research has been reported. Herein we describe the synergistic cocatalytic effect between carbon nanodots (CDots) and Co_3O_4, which promotes the photoelectrochemical water oxidation activity of the Fe_2O_3 photoanode with a 60 mV cathodically shifted onset potential. The C/Co_3O_4-Fe_2O_3 photoanode exhibits a photocurrent density of 1.48 mA cm^{-2} at 1.23 V (vs. reversible hydrogen electrode), 78% higher than that of the bare Fe_2O_3 photoanode. The slow reaction process on the single Co^{III}-OH site of the Co_3O_4 cocatalyst, oxidizing H_2O to H_2O_2 with two photogenerated holes, could be accelerated by the timely H_2O_2 oxidation to O_2 catalyzed on CDots.*

Hydrogen production via solar water splitting is one of the most promising approaches to develop sustainable energy resources.[1] Semiconductor photocatalysts with suitable band-gap structures, good charge-carrier conductivities, and fast surface reaction kinetics are desired to achieve high solar-energy conversion efficiencies.[2] The surface reaction kinetics of photocatalysts could be enhanced by integrating cocatalysts, which can provide surface reaction sites with lower overpotentials.[3] Moreover, cocatalysts could act as selective trapping sites for photogenerated electrons/holes and suppress the recombination of charge carriers.[4] Thus, strategies of cocatalysts loading have been extensively developed to enhance the activity of semiconductor photo-absorbers with slow surface reaction kinetics. Much attention has been paid to the water oxidation half reaction since it is regarded as the rate determining and kinetically unfavored process (with four electrons involved to produce one O_2 molecule).[5]

Cobalt-based compounds have been developed as cocatalysts for photocatalytic water oxidation.[6] Comparing with iridium and ruthenium oxides, cobalt-based materials are earth-abundant and cost-effective.[7] Cobalt phosphate (Co-Pi) showed a prominent promotive effect on the activity of hematite (α-Fe_2O_3) for photoelectrochemical water oxidation with a substantial cathodic onset potential shift and an enhanced photocurrent density.[8] It was demonstrated that the Co-Pi could increase the lifetime of photogenerated holes and retard the recombination of charge carriers.[9] The photocatalytic water-oxidation activity of Fe_2O_3 photoanode could also be effectively improved by integration of an inorganic Co_3O_4 cocatalyst.[10]

Metal-free materials are also investigated as cocatalysts for solar water splitting. Graphitic carbon nanodots (CDots) were demonstrated to enhance the photocatalytic water-oxidation activates of TiO_2 nanotube arrays,[11] ZnO nanowire arrays,[12] and $Ag_3PW_{12}O_{40}$ photocatalyst.[13] Most recently, a CDots/C_3N_4 composite photocatalyst showed an outstanding activity for solar water splitting with an overall solar-energy conversion efficiency of 2.0%.[14] It was proposed that the CDots performed as highly active catalysts for the decomposition of H_2O_2, which was considered as the intermediate spices from a two-step-two-electron water-splitting process on C_3N_4. Comparing with the one-step-four-electron water-splitting route, such a reaction pathway is kinetically favored, which leads to the high activity of the CDots/C_3N_4 photocatalyst.

Cocatalysts ranging from metal oxides to metal-free materials have been widely studied for improving the activity of semiconductor photocatalysts. However, relevant research mostly focuses on single-component cocatalyst, whose cocatalytic effect is restricted to the physical, chemical and electronic properties of the material. As complex processes are involved in the water-oxidation reaction, single cocatalyst can hardly realize the acceleration of all these processes simultaneously. Thus, to achieve better a performance it is desirable to fabricate a cocatalytic system with different functions for synergistic enhancement. Fe_2O_3 is selected to demonstrate the effectiveness of cocatalyst systems owing to its notoriously slow surface reaction kinetics for water oxidation.[15] By comparing the activity of Fe_2O_3 photoanodes with different cocatalysts (i.e., CDots, Co_3O_4, and both of them), we demonstrated that Co_3O_4 and CDot cocatalysts showed a synergistic cocatalytic effect. Ex situ detection of H_2O_2 from electrolyte was conducted to investigate the mechanism of the effect.

The Fe_2O_3 photoanode was prepared by a previously reported hydrothermal approach (see Supporting Information for experimental details).[16] The Fe_2O_3 photoanode obtained shows a one-dimensional wormlike structure (Fig-

[*] Dr. P. Zhang,[+] Prof. T. Wang,[+] X. Chang, Prof. L. Zhang, Prof. J. Gong
Key Laboratory for Green Chemical Technology of Ministry of Education, School of Chemical Engineering and Technology, Tianjin University, Collaborative Innovation Center of Chemical Science and Engineering
Tianjin 300072 (China)
E-mail: jlgong@tju.edu.cn

[+] These authors contributed equally to this work.

Supporting information and the ORCID identification number(s) for the author(s) of this article can be found under http://dx.doi.org/10.1002/anie.201600918.

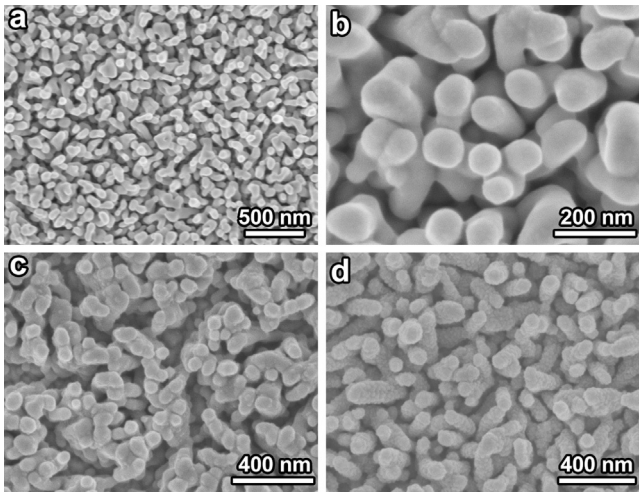

Figure 1. Scanning electron microscopy (SEM) images of a) Fe_2O_3, b) C-Fe_2O_3, c) Co_3O_4–Fe_2O_3, and d) C/Co_3O_4–Fe_2O_3 photoanodes.

ure 1a). The thickness of the Fe_2O_3 films is 224 ± 22 nm (Figure S1 in the Supporting Information). Upon the integration of CDots, the surface of Fe_2O_3 becomes slightly rougher (C-Fe_2O_3; Figure 1b). However, CDot particles could not be observed since their size is extremely small. Particulate Co_3O_4 is observed on the surface of the Co_3O_4–Fe_2O_3 photoanode (Figure 1c). When both CDots and Co_3O_4 were loaded onto the Fe_2O_3 photoanode its surface became rough with particles clearly shown on the surface (Figure 1d), which indicates the successful preparation of C/Co_3O_4–Fe_2O_3 photoanode.

Transmission electron microscopy (TEM) images were obtained to better illustrate the configurations of the cocatalysts on different photoanodes. CDot with a lattice spacing of 0.202 nm (corresponding to the (101) lattice planes of graphitic carbon) was tightly attached on the surface of C-Fe_2O_3 photoanode (Figure S2a). The CDot exhibits a size of about 5 nm. Fe_2O_3 is well crystalized showing a clear lattice with a spacing of 0.262 nm (corresponding to the (104) lattice planes of Fe_2O_3). The Co_3O_4 cocatalysts with a lattice spacing of 0.293 nm (corresponding to the (220) lattice planes of Co_3O_4) were loaded on Co_3O_4–Fe_2O_3 photoanode (Figure S2b). The Co_3O_4 particles have a size of about 8 nm. On C/Co_3O_4–Fe_2O_3 photoanode, CDots with a lattice spacing of 0.202 nm and Co_3O_4 with a lattice spacing of 0.244 nm (corresponding to the (311) lattice planes of Co_3O_4) are distributed without aggregation on the surface (indicated with white circles in Figure 2).[14] Moreover, the random loading leads to the two types of cocatalysts being adjacent to each other (Figure 2b), which accounts for their synergistic cocatalytic effect.

Only the characteristic X-ray diffraction (XRD) peaks of hematite at 36.3° and 64.6° could be observed for different samples owing to the relatively small sizes and low loading amounts of the cocatalysts (Figure S3).[17] However, the ultraviolet/visible (UV/Vis) light absorption spectra of different photoanodes reveal that the loading of CDots could enhance the light absorption of Fe_2O_3 photoanodes, while Co_3O_4 could only slightly improve the light-absorption ability

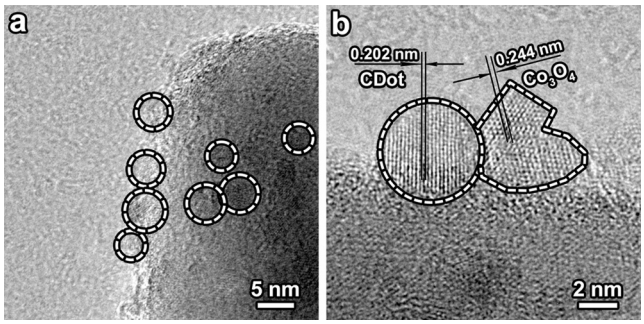

Figure 2. TEM images of C/Co_3O_4–Fe_2O_3 photoanodes at a) low and b) high magnification. White circles in (a) indicate CDots.

(Figure S4). As indicated by X-ray photoelectron spectroscopy (XPS), the O1s peaks at 531.2 eV for C-Fe_2O_3 and C/Co_3O_4–Fe_2O_3 photoanodes correspond to the -C−OH, -C=O, and O=C−O- groups on the surface of CDots (Figure S5a).[18] The XPS peaks at 796.4 eV and 780.4 eV for Co_3O_4–Fe_2O_3 and C/Co_3O_4–Fe_2O_3 photoanodes corresponds to the $Co2p_{1/2}$ and $Co2p_{3/2}$ spin-orbits in Co_3O_4, respectively (Figure S5c).[19] The peaks at 724.1 eV and 710.6 eV represent the $Fe2p_{1/2}$ and $Fe2p_{3/2}$ spin-orbits in Fe_2O_3,[20] which exhibit lower peak intensities without any peak shift upon the integration of cocatalysts (Figure S5b). This phenomenon indicates that the cocatalysts partly cover the surface of Fe_2O_3 photoanodes.

The activities for photocatalytic water oxidation of different photoanodes were examined by measuring the photocurrent density versus bias (J–V) curves in NaOH electrolyte (1M, pH 13.6) under simulated air mass 1.5 global (AM 1.5G) irradiation at 100 mW cm^{-2} (Figure 3a). The applied bias photon-to-current conversion efficiency (ABPE) and incident photon-to-current conversion efficiency (IPCE) of different photoanodes were also measured (Figure 3b,c). The IPCE spectra were collected with a bias of 1.23 V (vs. reversible hydrogen electrode (RHE)) and integrated over the AM 1.5G spectrum to obtain photocurrent densities, which are close to the values from J–V curves, confirming the accuracy of the results (Table S1).[21]

The as-prepared Fe_2O_3 photoanode exhibits a photocurrent density of 0.83 mA cm^{-2} at 1.23 V (vs. RHE). The onset potential (determined as the crossing point of a tangent to the inflection part of the photocurrent density with the dark current[22]) is about 0.85 V (vs. RHE), which is relatively low as a result of the partial removal of surface states by the high-temperature annealing.[23] The ABPE of Fe_2O_3 is 0.067% at 1.0 V (vs. RHE). The IPCE of Fe_2O_3 is about 20% in the 325–375 nm range. CDot cocatalysts do not show an obvious promotive effect, as the photocurrent density of C-Fe_2O_3 photoanode at 1.23 V (vs. RHE) does not change, and there is little change in the ABPE and the IPCE. However, the onset potential of the C-Fe_2O_3 photoanode shows a cathodic shift of 40 mV, which may be caused by the high conductivity of the CDots. The Co_3O_4 cocatalysts can enhance the activity of the Fe_2O_3 photoanode, leading to a photocurrent density of 1.23 mA cm^{-2} at 1.23 V (vs. RHE) as well as a 20 mV cathodic shift of the onset potential. The ABPE and the IPCE of Co_3O_4–Fe_2O_3 photoanode are 0.14% and 25% (at 375–

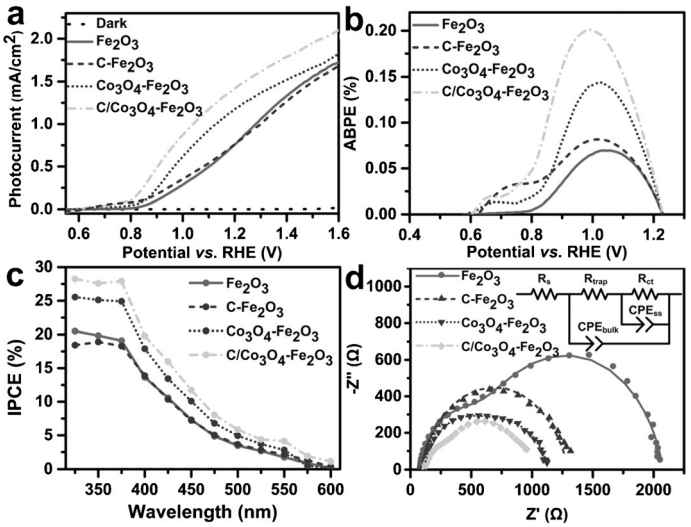

Figure 3. a) *J–V* curves, b) applied bias photon-to-current conversion efficiency (ABPE), c) incident photon-to-current conversion efficiency (IPCE), and d) electrochemical impedance spectroscopy (EIS) in Nyquist plots of Fe_2O_3, C-Fe_2O_3, Co_3O_4–Fe_2O_3, and C/Co_3O_4–Fe_2O_3 photoanodes. The symbols shows the measured data and the lines shows the fitting results in (d). Inset of (d) shows the equivalent circuit of the photoanodes.

325 nm), respectively. When CDots and Co_3O_4 are loaded simultaneously, the activity is extensively enhanced. The photocurrent density of the C/Co_3O_4–Fe_2O_3 photoanode is 1.48 mA cm^{-2} at 1.23 V (vs. RHE), which is 78% higher than that of the bare Fe_2O_3 photoanode. This enhancement is the largest reported value at 1.23 V (vs. RHE) for the cocatalyst strategy in non-sacrificial photoelectrochemical water oxidation by Fe_2O_3 photoanodes. Moreover, the onset potential shows a cathodic shift of 60 mV, indicating a lower overpotential for water oxidation as a result of the synergistic cocatalytic effect. The onset potential of the Fe_2O_3 photoanode would be further reduced by the optimization of the loading ratios and the amounts of different cocatalysts as well as the strengthening of the connection between the cocatalysts and the Fe_2O_3 photoanode. The ABPE of the C/Co_3O_4–Fe_2O_3 photoanode is 0.20% at 1.0 V (vs. RHE), which is 2.46 times that of the bare Fe_2O_3 photoanode. Moreover, the IPCE is about 28% in the 375–325 nm range.

Electrochemical impedance spectroscopy (EIS) characterization was conducted under AM 1.5G (Figure 3d). Two clear semicircles are observed for the bare Fe_2O_3 photoanode, indicating the existence of two capacitances.[24] Thus, a typical equivalent circuit model was used to fit the EIS data (inset of Figure 3d), which involved a series resistors (R_s), a surface states charge trapping resistance (R_{trap}), a charge transfer resistance (R_{ct}), a depletion layer capacitance (CPE_{bulk}), and a surface states trapped charge capacitance (CPE_{ss}). Constant phase elements were used owning to the non-ideal feature of the capacitances caused by the nanostructure of the electrodes.[25] The fitting results of R_{trap} for different photoanodes are similar (Table 1), because the Fe_2O_3 substrates of different samples are alike. However, the values of R_{ct} change dramatically when Fe_2O_3 is loaded with cocatalysts. Co_3O_4 shows a better cocatalytic effect than the CDots, as reflected by the lower charge-transfer resistance of Co_3O_4–Fe_2O_3 photoanode, which is in accordance with the *J–V* curves. When both CDots and Co_3O_4 cocatalysts are loaded on to Fe_2O_3, the value of R_{ct} decreases further, demonstrating their synergistic cocatalytic effect.

As the synergistic cocatalytic effect between CDots and Co_3O_4 has been demonstrated through the activity tests and the EIS characterization, it is worthwhile understanding the mechanism of such a synergistic effect. The intermediates of water oxidation on Co_3O_4 had been investigated through time-resolved Fourier-transform infrared spectroscopy, suggesting that two kinds of reaction sites exist on the surface.[26] The fast-reaction site, containing two linked Co^{III}–OH groups, could directly oxidize H_2O to molecular O_2 with four photogenerated holes (Figure 4a). On the other hand, the single Co^{III}–OH slow-reaction site is initially oxidized to Co^{IV}=O by one photogenerated hole. After the attack and deprotonation of H_2O molecule, the slow-reaction site changes to Co^{II}–OOH. Then another H_2O molecule in the electrolyte reacts with Co^{II}–OOH to form H_2O_2,[27] when Co^{II}–OOH is oxidized by the second photogenerated hole to restore the Co^{III}–OH site. Thus, a complete cycle is established to oxidize H_2O to H_2O_2 at the slow-reaction site of Co_3O_4. Recently, CDots have been shown to be an

Table 1: EIS Fitting results of R_{trap} and R_{ct} for Fe_2O_3, C-Fe_2O_3, Co_3O_4–Fe_2O_3, and C/Co_3O_4–Fe_2O_3 photoanodes.

Sample	Fe_2O_3	C-Fe_2O_3	Co_3O_4–Fe_2O_3	C/Co_3O_4–Fe_2O_3
R_{trap} [Ω]	670±10	592±139	600±10	678±43
R_{ct} [Ω]	1330±13	690±147	417±12	230±37

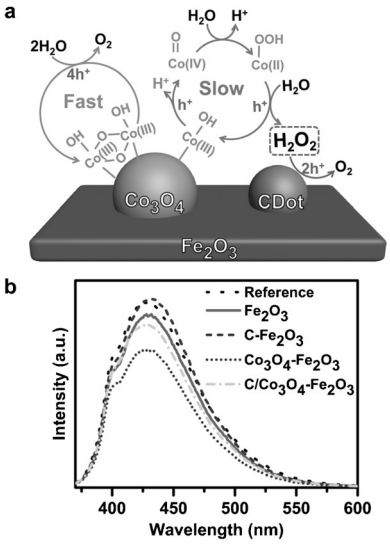

Figure 4. a) Schematic illustration of the fast/slow reaction processes on Co_3O_4 cocatalyst and the two-step-two-electron reaction pathway for photocatalytic water oxidation on the C/Co_3O_4-Fe_2O_3 photoanode. b) Photoluminescence (PL) spectra of the scopoletin assay of the electrolytes after solar water-splitting reactions with different photoanodes.

excellent catalyst for H_2O_2 decomposition.[14,28] Therefore, the H_2O_2 formed at the slow-reaction site on Co_3O_4 is further oxidized to molecular O_2 on CDots, which results in the two-step-two-electron reaction pathway for water oxidation (Figure 4a). The prompt consumption of H_2O_2 in the two-step-two-electron reaction pathway causes the acceleration of the slow-reaction process on Co_3O_4. Comparing with the four-electron water-oxidation reaction, the two-step-two-electron reaction pathway is kinetically favored, requiring a lower concentration of photogenerated holes on the surface.[29] This two-step-two-electron reaction pathway explains the synergistic cocatalytic effect between CDots and Co_3O_4. To confirm this hypothesis, ex situ detection of the H_2O_2 in the reaction electrolyte was conducted.

As the amount of H_2O_2 in the electrolyte is low, a sensitive chemiluminescence detection method by scopoletin assay was performed.[30] The fluorescent scopoletin could be oxidized by H_2O_2 at the presence of horseradish peroxidase, leading to the loss of its fluorescence.[31] Thus, the higher intensity of the emission peak for scopoletin at 430 nm in the photoluminescence (PL) spectra indicates a lower concentration of H_2O_2 in the reaction electrolyte, and vice versa (Figure 4b). Comparing the results between the reference (experiment without electrodes, i.e., only electrolyte was irradiated by light) and the Fe_2O_3 photoanode, it can be inferred that a small amount of H_2O_2 is produced during the photoelectrochemical water oxidation on Fe_2O_3. When only CDot cocatalyst is loaded on Fe_2O_3, the increased intensity of the emission peak indicates that the H_2O_2 produced could be decomposed in the presence of CDots, confirming their catalytic effect for H_2O_2 decomposition. However, in the case of the Co_3O_4–Fe_2O_3 photoanode, much more H_2O_2 is detected to quench the fluorescence, confirming the existence of the slow-reaction site on Co_3O_4. When both CDots and Co_3O_4 are loaded on the Fe_2O_3 photoanode, the intensity of the emission peak rises back to a similar level as for bare Fe_2O_3 photoanode, which shows that the H_2O_2 produced on the Co_3O_4 cocatalyst is further oxidized on the CDot cocatalysts. Thus, the two-step-two-electron reaction path way and the synergistic cocatalytic effect of CDots and Co_3O_4 are confirmed by this chemiluminescence detection of H_2O_2 produced during photoelectrochemical water oxidation.

In summary, we have demonstrated the synergistic cocatalytic effect between CDots and Co_3O_4 to enhance the activity of the Fe_2O_3 anode for photoelectrochemical water oxidation. When the two cocatalysts are loaded onto the anode, a kinetically favored two-step-two-electron reaction partway is established. Initially, the water molecule is oxidized to H_2O_2 at the slow-reaction site on Co_3O_4. The H_2O_2 produced is then further oxidized to O_2 on the CDot cocatalysts. Thus, the slow reaction process on Co_3O_4 is accelerated. The kinetically favored two-step-two-electron reaction partway and the enhanced surface reaction rate result in the improved solar water-oxidation activity of the Fe_2O_3 photoanodes. The discovery of this synergistic effect between different cocatalysts can help design effective cocatalytic systems with multiple functional components, an effect which is also applicable to other energy conversion applications.

Acknowledgements

We thank the National Natural Science Foundation of China (21525626, U1463205, 21222604, and 51302185), Specialized Research Fund for the Doctoral Program of Higher Education (20120032110024 and 20130032120018), the Scientific Research Foundation for the Returned Overseas Chinese Scholars (MoE), the Program of Introducing Talents of Discipline to Universities (B06006), and the Natural Science Foundation of Tianjin City (13JCYBJC37000) for financial support.

Keywords: carbon nanodots · Co_3O_4 · cocatalysts · iron · water splitting

How to cite: *Angew. Chem. Int. Ed.* **2016**, *55*, 5851–5855
Angew. Chem. **2016**, *128*, 5945–5949

[1] a) M. G. Walter, E. L. Warren, J. R. McKone, S. W. Boettcher, Q. Mi, E. A. Santori, N. S. Lewis, *Chem. Rev.* **2010**, *110*, 6446–6473; b) X. Chen, S. Shen, L. Guo, S. S. Mao, *Chem. Rev.* **2010**, *110*, 6503–6570; c) T. Wang, J. Gong, *Angew. Chem. Int. Ed.* **2015**, *54*, 10718–10732; *Angew. Chem.* **2015**, *127*, 10866–10881.

[2] a) Y. Ma, X. Wang, Y. Jia, X. Chen, H. Han, C. Li, *Chem. Rev.* **2014**, *114*, 9987–10043; b) P. Zhang, J. Zhang, J. Gong, *Chem. Soc. Rev.* **2014**, *43*, 4395–4422.

[3] J. Ran, J. Zhang, J. Yu, M. Jaroniec, S. Z. Qiao, *Chem. Soc. Rev.* **2014**, *43*, 7787–7812.

[4] J. Yang, D. Wang, H. Han, C. Li, *Acc. Chem. Res.* **2013**, *46*, 1900–1909.

[5] J. D. Blakemore, R. H. Crabtree, G. W. Brudvig, *Chem. Rev.* **2015**, *115*, 12974–13005.

[6] X. Chang, T. Wang, P. Zhang, J. Zhang, A. Li, J. Gong, *J. Am. Chem. Soc.* **2015**, *137*, 8356–8359.

[7] J. Wang, W. Cui, Q. Liu, Z. Xing, A. M. Asiri, X. Sun, *Adv. Mater.* **2015**, *28*, 215–230.

[8] a) D. K. Zhong, J. Sun, H. Inumaru, D. R. Gamelin, *J. Am. Chem. Soc.* **2009**, *131*, 6086–6087; b) K. J. McDonald, K.-S. Choi, *Chem. Mater.* **2011**, *23*, 1686–1693.

[9] B. Klahr, S. Gimenez, F. Fabregat-Santiago, J. Bisquert, T. W. Hamann, *J. Am. Chem. Soc.* **2012**, *134*, 16693–16700.

[10] L. Xi, P. D. Tran, S. Y. Chiam, P. S. Bassi, W. F. Mak, H. K. Mulmudi, S. K. Batabyal, J. Barber, J. S. C. Loo, L. H. Wong, *J. Phys. Chem. C* **2012**, *116*, 13884–13889.

[11] X. Zhang, F. Wang, H. Huang, H. Li, X. Han, Y. Liu, Z. Kang, *Nanoscale* **2013**, *5*, 2274–2278.

[12] C. X. Guo, Y. Dong, H. B. Yang, C. M. Li, *Adv. Energy Mater.* **2013**, *3*, 997–1003.

[13] J. Liu, H. Zhang, D. Tang, X. Zhang, L. Yan, Y. Han, H. Huang, Y. Liu, Z. Kang, *ChemCatChem* **2014**, *6*, 2634–2641.

[14] J. Liu, Y. Liu, N. Liu, Y. Han, X. Zhang, H. Huang, Y. Lifshitz, S.-T. Lee, J. Zhong, Z. Kang, *Science* **2015**, *347*, 970–974.

[15] a) K. Sivula, F. Le Formal, M. Grätzel, *ChemSusChem* **2011**, *4*, 432–449; b) I. Cesar, A. Kay, J. A. Gonzalez Martinez, M. Grätzel, *J. Am. Chem. Soc.* **2006**, *128*, 4582–4583; c) Y. Lin, G. Yuan, S. Sheehan, S. Zhou, D. Wang, *Energy Environ. Sci.* **2011**, *4*, 4862.

[16] L. Vayssieres, N. Beermann, S.-E. Lindquist, A. Hagfeldt, *Chem. Mater.* **2001**, *13*, 233–235.

[17] B. M. Klahr, A. B. F. Martinson, T. W. Hamann, *Langmuir* **2011**, *27*, 461–468.

[18] H. Sun, A. Zhao, N. Gao, K. Li, J. Ren, X. Qu, *Angew. Chem. Int. Ed.* **2015**, *54*, 7176–7180; *Angew. Chem.* **2015**, *127*, 7282–7286.

[19] B. Varghese, C. H. Teo, Y. Zhu, M. V. Reddy, B. V. R. Chowdari, A. T. S. Wee, V. B. C. Tan, C. T. Lim, C. H. Sow, *Adv. Funct. Mater.* **2007**, *17*, 1932 – 1939.
[20] R. Morrish, M. Rahman, J. M. D. MacElroy, C. A. Wolden, *ChemSusChem* **2011**, *4*, 474 – 479.
[21] Y. Li, L. Zhang, A. Torres-Pardo, J. M. González-Calbet, Y. Ma, P. Oleynikov, O. Terasaki, S. Asahina, M. Shima, D. Cha, L. Zhao, K. Takanabe, J. Kubota, K. Domen, *Nat. Commun.* **2013**, *4*, 2556.
[22] F. Le Formal, N. Tétreault, M. Cornuz, T. Moehl, M. Grätzel, K. Sivula, *Chem. Sci.* **2011**, *2*, 737 – 743.
[23] O. Zandi, T. W. Hamann, *J. Phys. Chem. Lett.* **2014**, *5*, 1522 – 1526.
[24] B. Klahr, T. Hamann, *J. Phys. Chem. C* **2014**, *118*, 10393 – 10399.
[25] T. Lopes, L. Andrade, F. Le Formal, M. Grätzel, K. Sivula, A. Mendes, *Phys. Chem. Chem. Phys.* **2014**, *16*, 16515.
[26] M. Zhang, M. de Respinis, H. Frei, *Nat. Chem.* **2014**, *6*, 362 – 367.
[27] G. Duca, *Homogeneous Catalysis with Metal Complexes*, Springer, Berlin, **2012**.
[28] H. Sun, N. Gao, K. Dong, J. Ren, X. Qu, *ACS Nano* **2014**, *8*, 6202 – 6210.
[29] F. Le Formal, E. Pastor, S. D. Tilley, C. A. Mesa, S. R. Pendlebury, M. Grätzel, J. R. Durrant, *J. Am. Chem. Soc.* **2015**, *137*, 6629 – 6637.
[30] H. Perschke, E. Broda, *Nature* **1961**, *190*, 257 – 258.
[31] J. T. Corbett, *J. Biochem. Biophys. Methods* **1989**, *18*, 297 – 307.

Received: January 27, 2016
Published online: March 24, 2016

